NJC

PAPER

View Article Online
View Journal | View Issue

Check for updates

Cite this: *New J. Chem.*, 2025, **49**, 17997

# Activating harmful small molecules under mild conditions: theoretical insights into cinchonine-based valorization of $CO_2$, $CS_2$, and COS

Lucia Invernizzi,[a] Caterina Damiano,*[a] Gabriele Manca*[b] and Emma Gallo[a]

DFT calculations have been employed to deeply investigate the mechanism of $CO_2$ cycloaddition to aziridines catalyzed by cinchonine hydrochloride salt, forming oxazolidin-2-ones under ambient conditions (room temperature, 0.1 MPa $CO_2$). Computed energy barriers align with experimental observations and support a dual activation mechanism involving hydrogen bonding and nucleophilic attack at the aziridine carbon atom. The theoretical study also accounts for the observed regioselectivity, rationalizing the preference for nucleophilic attack at the more substituted aziridine carbon atom. Consistent with experimental findings, the calculations reveal that the reaction efficiency is influenced by the nature of the substituent at the aziridine nitrogen atom, explaining the lack of reactivity observed with *N*-aryl aziridines due to steric and electronic factors that hamper the reaction. Furthermore, the DFT study suggests that COS and $CS_2$ can be activated for analogous cycloaddition reactions. Although these transformations involve higher energy barriers compared to $CO_2$ cycloaddition, the formation of oxazolidin-2-thiones and thiazolidin-2-thiones is predicted to be feasible under slightly elevated temperatures (for $CS_2$) or near-ambient conditions (for COS). These findings highlight the potential of cinchonine hydrochloride salt as an efficient, biocompatible and cost-effective catalyst for the sustainable valorization of small harmful molecules under mild conditions.

Received 6th August 2025,
Accepted 11th September 2025

DOI: 10.1039/d5nj03189c

rsc.li/njc

Open Access Article. Published on 11 September 2025. Downloaded on 1/23/2026 4:32:47 PM.
This article is licensed under a Creative Commons Attribution 3.0 Unported Licence.

## Introduction

The activation of small molecules has long been a central theme in chemical research, driven by the challenge of breaking strong bonds in simple, thermodynamically stable species. Historically, much of this work has focused on inert molecules such as $N_2$, $O_2$ and $CH_4$, which are starting materials in processes like nitrogen fixation, oxidation reactions, and hydrocarbon functionalization.[1,2] During the last decades, scientific interest has progressively moved toward carbon dioxide. Although $CO_2$ is similarly unreactive, it presents a distinctive combination of scientific and environmental urgency. Its massive atmospheric abundance, mainly due to anthropogenic emissions, and its well-established role in global warming have made its activation a priority in the context of sustainable chemistry. As a result, $CO_2$ is now viewed not only as a waste product but also as a potential carbon feedstock, whose efficient transformation could contribute to both climate mitigation and resource circularity.

Advances in catalytic[3–5] and electrochemical methods[6–8] have enabled the efficient conversion of $CO_2$ into a variety of useful chemicals[9] and fuels[10] such as carbon monoxide, formic acid, methanol, methane, and a range of value-added compounds. In light of the development of a circular and sustainable economy, the establishment of new and efficient processes for $CO_2$ valorization has become interesting for the synthesis of fine chemicals. One particularly intriguing reaction is the 100% atom-efficient cycloaddition of $CO_2$ into organic substrates, such as epoxides[11,12] and aziridines,[13–20] to produce high-value chemicals like cyclic carbonates and oxazolidin-2-ones, respectively, which have several applications including as pharmaceutical agents.[21–23] Classic $CO_2$ activation typically requires the co-presence of an electrophilic and a nucleophilic promoter. In the synthesis of oxazolidin-2-ones, the electrophile, generally a metal center, interacts with the nitrogen aziridine atom to render one of the two carbon atoms more susceptible to nucleophilic attack. The consequent cleavage of the C–N bond transfers electron density to the nitrogen atom, which in turn becomes capable of activating the $CO_2$ molecule (Scheme 1). The need for both electrophilic and nucleophilic functionalities led to the development of various binary and

[a] *Department of Chemistry, University of Milan, Via C. Golgi 19, 20133 Milan, Italy. E-mail: caterina.damiano@unimi.it*
[b] *Istituto di Chimica dei Composti Organo Metallici – CNR-ICCOM Sede Secondaria di Bari, c/o Dipartimento di Chimica, Università degli Studi di Bari, Via Orabona 4, 70126 Bari, Italy. E-mail: gmanca@iccom.cnr.it*

Open Access Article. Published on 11 September 2025. Downloaded on 1/23/2026 4:32:47 PM.
This article is licensed under a Creative Commons Attribution 3.0 Unported Licence.

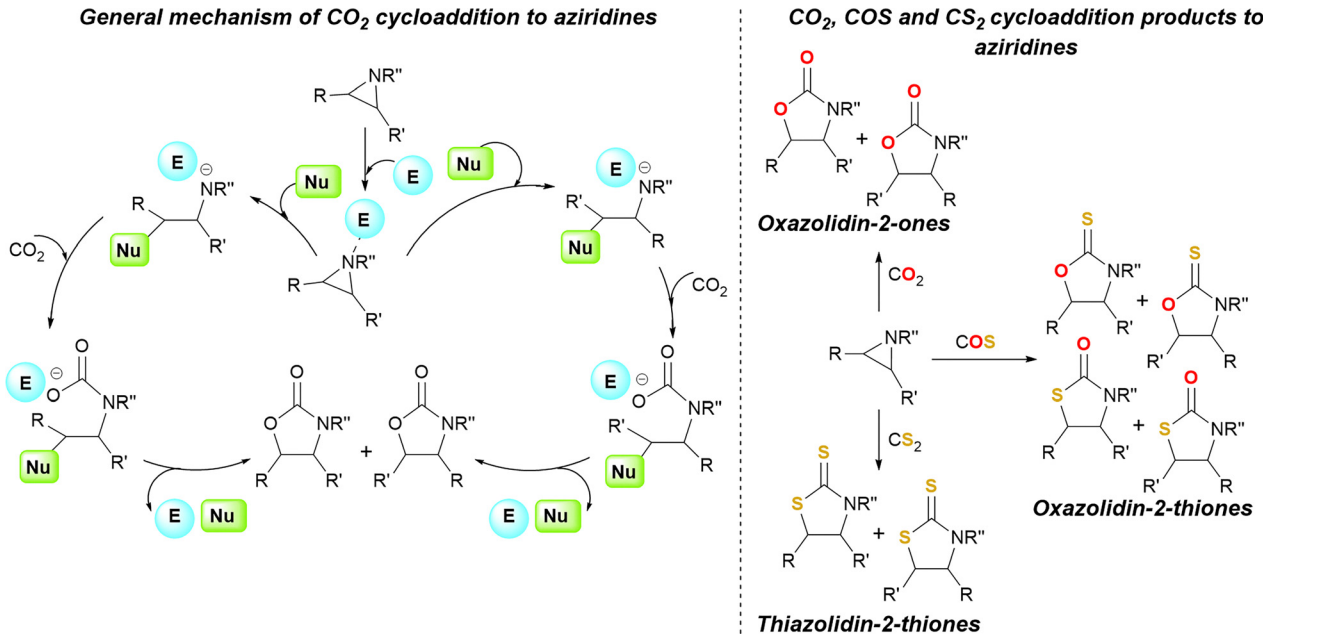


Scheme 1 General reaction mechanism of $CO_2$ cycloaddition to aziridines (left); $CO_2$, COS and $CS_2$ cycloaddition products to aziridines (right).

bifunctional metal-based catalysts for the $CO_2$ cycloaddition to aziridines.[4–10,13] More recently, metal-free systems,[14,15,18,19,24] which integrate both functional components enabling efficient aziridine activation and ring-opening without the use of external metal catalysts, have also been extensively developed.

Although $CO_2$ has received widespread attention as a platform molecule for sustainable synthesis, its thio-analogues, carbon disulfide ($CS_2$) and carbonyl sulfide (COS), have remained largely overlooked.

Since the early 1970s, when the reactivity of $CS_2$ toward aziridines was first investigated,[25,26] research on COS and $CS_2$ has primarily focused on their interactions with metal complexes.[27,28] Only in recent years, the interest in these triatomic molecules has expanded, with growing attention to their cycloaddition reactions with epoxides and aziridines, particularly *via* metal–organic framework (MOF)-based catalytic systems in combination with nucleophilic co-catalysts.[29–32] The limited experimental examples reported for the $CS_2$ cycloaddition to aziridines rely on expensive binary systems involving amidato divalent lanthanide complexes, among which the most active is represented by the europium derivative used in combination with DBU (1,8-diazabicyclo[5.4.0]undec-7-ene).[29] Other examples include a cerium-based framework,[30] a porous 3D cobalt–organic framework assembled by [$Co_{15}$] and [$Co_{18}$] nanocages[31] and a 3D material assembled by twisted cylindrical [$Dy_{24}$] cages.[32] In all cases, TBAB (tetrabutylammonium bromide) was the co-catalyst; either the metal centre or the positive channel of the MOF-based material acts as a Lewis acid to activate the aziridine, while the external nucleophile promotes the ring-opening reaction enabling $CS_2$ insertion and product formation. To date, no examples of active bifunctional organocatalytic systems have been reported. The above-described behavior aligns with the structural and electronic similarities between COS, $CS_2$, and $CO_2$, highlighting their potential for analogous activation and transformation pathways.[27,29,33] It is important to note that $CS_2$ and COS not only cause environmental effects but can also contribute to various health disorders, particularly affecting the human reproductive and nervous systems.[34,35] Therefore, rather than eliminating them through traditional combustion methods, treating and reusing these compounds as carbon and sulfur resources offers an attractive alternative to reduce the presence of toxic sulfur-containing pollutants in the atmosphere. In this view, $CS_2$ and COS could serve as valuable C1-building blocks for the synthesis of sulfur-containing heterocycles,[36–38] such as thiazolidin-2-thiones and oxazolidin-2-thiones (Scheme 1), and other functionalized materials,[39] offering new opportunities in the field of small-molecule activation and sustainable sulfur chemistry.

It is important to underline that the activation of small molecules, such as $CO_2$, $CS_2$, and COS, should occur under mild reaction conditions to ensure a favorable balance between the energy required for the transformation and the amount of $CO_2$ effectively utilized. If harsh conditions are employed, such as high temperatures, elevated pressures, or energy-intensive inputs, the environmental benefit of using these molecules as feedstocks may be offset by additional $CO_2$ emissions generated during the process. For this reason, the development of catalytic systems capable of operating efficiently under ambient or near-ambient conditions is essential to maximize the net carbon benefit and make these transformations truly viable from both an energetic and environmental standpoint.

Given the growing demand for low-toxicity synthetic procedures, the use of eco-friendly bifunctional organocatalysts has become increasingly attractive. Recently, we reported a combined experimental and computational investigation of the catalytic properties of the metal-free *bis*-protonated porphyrin

 This journal is © The Royal Society of Chemistry and the Centre National de la Recherche Scientifique 2025

Open Access Article. Published on 11 September 2025. Downloaded on 1/23/2026 4:32:47 PM.
This article is licensed under a Creative Commons Attribution 3.0 Unported Licence.

$TPPH_4Cl_2$ (TPP = dianion of tetraphenylporphyrin) in promoting the cycloaddition of $CO_2$ into *N*-alkyl aziridines to produce *N*-alkyl oxazolidin-2-ones at 100 °C and 1.2 MPa of $CO_2$ pressure.[16] Computational analysis revealed that the reaction occurred, thanks to porphyrin/aziridine synergic $CO_2$ activation in which the protonated core of porphyrin acts, by establishing hydrogen bonding with the $CO_2$ oxygen atom, as an electrophilic center to facilitate the nucleophilic attack of the aziridine nitrogen atom to the $CO_2$ carbon atom. The study paved the way for developing other bifunctional organocatalytic systems, bearing the same nucleophilic moiety (chloride anion) but different electrophilic $NH^+$-containing species, to promote the synthesis of *N*-alkyl oxazolidin-2-ones under milder experimental conditions.[40] In this context, some of us recently published a study on the catalytic activity of hydrochloride salts of DBU, quinine, and cinchonine,[40] which were active at room temperature and 0.1 MPa of $CO_2$ pressure. In view of the very good results achieved, we decided to investigate the electronic/energetic features of the mechanism of these reactions by using DFT calculations. In addition, the potential catalytic activity of cinchonine hydrochloride salt to promote the cycloaddition of other triatomic harmful molecules such as $CS_2$ and COS has been investigated *in silico*. The obtained computational results pave the way for developing future efficient and eco-compatible catalytic processes for the synthesis of fine chemicals by recycling waste.

## Results and discussion

### Cycloaddition of $CO_2$ to 1-butyl-2-phenylaziridine ($\mathbf{1_{butyl}}$) promoted by cinchonine hydrochloride (3)

In light of remarkable data published for the synthesis *N*-alkyl oxazolidin-2-ones under mild experimental conditions,[40] detailed computational analysis was carried out on the model $CO_2$ cycloaddition to 1-butyl-2-phenylaziridine ($\mathbf{1_{butyl}}$) yielding 3-butyl-5-phenyl oxazolidin-2-ones ($\mathbf{2A_{butyl}}$ + $\mathbf{2B_{butyl}}$) (Scheme 2), catalyzed by the naturally derived cinchonine hydrochloride salt (**3**). Although particular emphasis was placed on elucidating the reaction mechanism catalyzed by **3**, the mechanisms involving hydrochloride salts of DBU and quinine, organocatalysts **4** and **5** respectively, were also investigated and the collected data are reported in the SI. The structures of **3**, **4**, and **5** organocatalysts were optimized at the B97D-DFT level of theory,[41] and are shown in Fig. 1. The solvent effects have been taken into account by using the CPCM model[42,43] for acetonitrile that is the solvent employed in experimental studies already published on the $CO_2$ cycloaddition to aziridines.[40] Additional methodological details are provided in the SI.

According to the published experimental results,[40] 1-butyl-2-phenylaziridine ($\mathbf{1_{butyl}}$) was chosen as the model substrate to investigate the catalytic mechanism of the reaction promoted by **3**, and $CH_3CN$ was the modeled reaction solvent.

Drawing from prior data on the $TPPH_4Cl_2$-mediated reaction,[16] the first step of the computational analysis focused on the possible formation of adduct $\mathbf{6_{butyl}}$ in which $CO_2$ is positioned between hydrochloride salt **3** and aziridine $\mathbf{1_{butyl}}$. As shown in Fig. 2, $\mathbf{6_{butyl}}$ was computationally identified with a free energy cost of +15.0 kcal $mol^{-1}$ resulting from a balance between the favorable enthalpic contribution of −6.5 kcal $mol^{-1}$ and a severe unfavorable entropic contribution. The local electrophilicity index ($\omega_K^+$) of the two aziridine carbon atoms, namely C2 and C3, was estimated by using the method developed by Domingo *et al.*[44]

The calculations revealed that the $\omega_K^+$ value for C2 is twofold higher than that of C3, suggesting a more favored nucleophilic attack at C2 rather than at the C3 carbon atom. This is in line with the experimentally observed reaction regioselectivity,[40] as 3-butyl-5-phenyloxazolidin-2-one (compound $\mathbf{2A_{butyl}}$ in Scheme 2) was always detected as the major isomer. Consequently, the mechanism yielding isomer $\mathbf{2B_{butyl}}$, deriving from the nucleophilic attack on C3, was not further studied by DFT calculations.

In adduct $\mathbf{6_{butyl}}$, aziridine nitrogen atom N2 acts as a nucleophile toward $CO_2$, which loses its linearity with the O–C1–O angle reduced to 135°, as confirmed by the appearance of an IR-active vibration at 1759 $cm^{-1}$, associated with the

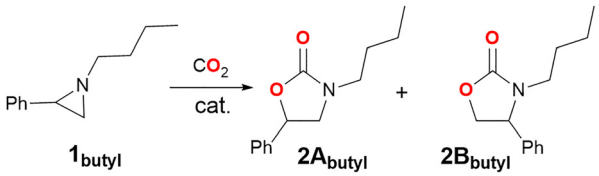


Scheme 2 Synthesis of 3-butyl-5-phenyloxazolidin-2-ones $\mathbf{2A_{butyl}}$ and $\mathbf{2B_{butyl}}$ by $CO_2$ cycloaddition to 1-butyl-2-phenylaziridine ($\mathbf{1_{butyl}}$).

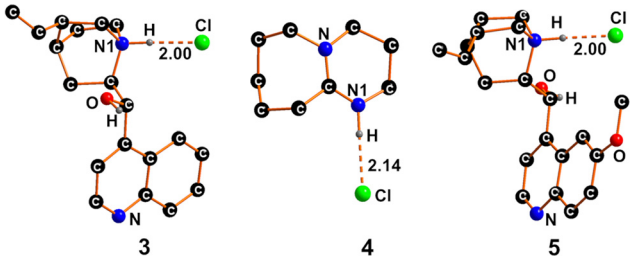


Fig. 1 Optimized structure of hydrochloride salts **3**, **4** and **5**. The hydrogen atoms were hidden for the sake of clarity, except for those linked to heteroatoms. Selected distances are given in Å.

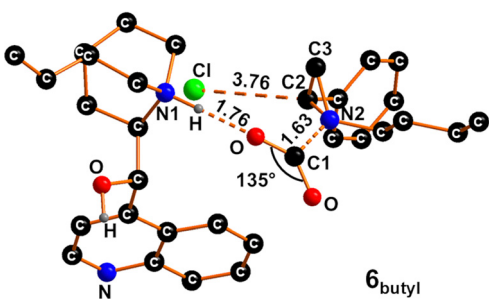


Fig. 2 Optimized structure of adduct $\mathbf{6_{butyl}}$. The hydrogen atoms were hidden for the sake of clarity, except for those linked to a heteroatom. Selected distances are given in Å and O–C1–O angle in degrees (°).

Open Access Article. Published on 11 September 2025. Downloaded on 1/23/2026 4:32:47 PM.
This article is licensed under a Creative Commons Attribution 3.0 Unported Licence.

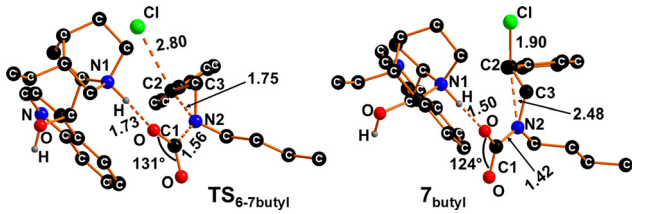


Fig. 3 Optimized structure of transition state $\mathbf{TS_{6\text{-}7butyl}}$ and intermediate $\mathbf{7_{butyl}}$. The hydrogen atoms were hidden for the sake of clarity, except for those linked to a heteroatom. Selected distances are given in Å and O–C1–O angle in degrees (°).

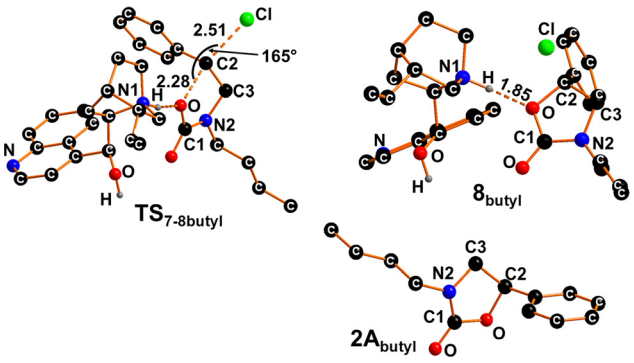


Fig. 4 Optimized structure of transition state $\mathbf{TS_{7\text{-}8butyl}}$, intermediate $\mathbf{8_{butyl}}$ and product $\mathbf{2A_{butyl}}$. The hydrogen atoms were hidden for the sake of clarity, except for those linked to a heteroatom. Selected distances are given in Å and O–C1–O angle in degrees (°).

asymmetric stretching of the C–O bonds. The chloride anion remains distant from the C2 center, with a Cl···C2 distance of 3.76 Å whose reduction to 2.80 Å revealed the presence of a transition state, designated $\mathbf{TS_{6\text{-}7butyl}}$ (Fig. 3).

In $\mathbf{TS_{6\text{-}7butyl}}$, the approaching chloride anion weakens the N2–C2 bond, which is elongated by 0.15 Å compared to adduct $\mathbf{6_{butyl}}$. This facilitates the initial shift of electron density toward the aziridine nitrogen N2, enhancing its nucleophilicity toward $CO_2$. This effect is further supported by a 0.07 Å shortening of the N2···C1 distance and a more pronounced bending of the $CO_2$ moiety, with the O–C–O angle reduced by 4° with respect to adduct $\mathbf{6_{butyl}}$. From an energetic perspective, the transition from $\mathbf{6_{butyl}}$ to $\mathbf{TS_{6\text{-}7butyl}}$ involves an estimated free energy barrier of +4.3 kcal mol$^{-1}$. The transition-state nature of $\mathbf{TS_{6\text{-}7butyl}}$ was confirmed by the presence of a single imaginary frequency at −170 cm$^{-1}$, corresponding to the approach of the chloride ion to the C2 atom and the complete cleavage of the C2–N2 bond. Following $\mathbf{TS_{6\text{-}7butyl}}$, the system evolves toward the minimum-energy structure $\mathbf{7_{butyl}}$ (Fig. 3) that displays the complete formation of the C2–Cl bond (1.90 Å) and the corresponding cleavage of the N2···C2 bond (2.48 Å). The C1–N2 bond is also fully formed, with a length of 1.42 Å. The formation of intermediate $\mathbf{7_{butyl}}$ was estimated to be exergonic, with a free energy change of −12.6 kcal mol$^{-1}$. At this point, the electron density originally localized on the N2 center has shifted toward the oxygen atoms of the original $CO_2$ moiety, leading to a strengthening of the O···H hydrogen bond, as indicated by a 0.23 Å shortening compared to the corresponding distance in $\mathbf{TS_{6\text{-}7butyl}}$.

As confirmed by this O···H shortening, the oxygen atom of intermediate $\mathbf{7_{butyl}}$ becomes electron-rich and capable of performing a nucleophilic attack to the C2 center yielding oxazolidin-2-one $\mathbf{2A_{butyl}}$ by a ring-closure step and the regeneration of catalyst **3**. Intermediate $\mathbf{8_{butyl}}$ (Fig. 4) was achieved through the formation of the transition state $\mathbf{TS_{7\text{-}8butyl}}$, whose structure was computationally identified (Fig. 4).

In $\mathbf{TS_{7\text{-}8butyl}}$, the O–C2–Cl moiety adopts a *quasi*-linear arrangement with an angle of 165°, and the C2 atom approaches a *quasi*-planar geometry. The nucleophilic approach of oxygen atom to C2 initiates the displacement of the chloride ion with an associated free energy barrier of +7.4 kcal mol$^{-1}$. The transition state nature of $\mathbf{TS_{7\text{-}8butyl}}$ is supported by the presence of a single imaginary frequency at −216 cm$^{-1}$, corresponding to the formation of the O–C2 bond and the cleavage of the C2–Cl bond. Subsequently, intermediate $\mathbf{8_{butyl}}$ is obtained with a free energy gain of −20.1 kcal mol$^{-1}$ (Fig. 4).

The complete release of 3-butyl-5-phenyloxazolidin-2-one ($\mathbf{2A_{butyl}}$) from $\mathbf{8_{butyl}}$ is exergonic by −5.1 kcal mol$^{-1}$ accompanied by the restoration of the salt **3**, able to perform the activation of a new aziridine moiety. The overall free energy gain, associated with the complete catalytic cycloaddition of $CO_2$ to 1-butyl-2-phenyl aziridine $\mathbf{1_{butyl}}$ yielding $\mathbf{2A_{butyl}}$, was estimated to be exergonic by −11.2 kcal mol$^{-1}$ (Fig. 5).

The energy profile of the reaction (Fig. 5) reveals that the largest cost for the synthesis of $\mathbf{2A_{butyl}}$ is +19.3 kcal mol$^{-1}$, with the main disfavoring contribution associated with the formation of the initial adduct $\mathbf{6_{butyl}}$. For comparison purposes, the cycloaddition of $CO_2$ to $\mathbf{1_{butyl}}$ was also investigated in the presence of catalysts **4** and **5**. The free energy pathways for the three catalytic processes are reported in the SI (Fig. S1). No substantial changes in free energy were identified, except for the free energy stabilization of compounds analogous to intermediate $\mathbf{7_{butyl}}$, namely $\mathbf{7'_{butyl}}$ (involving catalyst **4**) and $\mathbf{7''_{butyl}}$ (involving catalyst **5**) within 6 kcal mol$^{-1}$. The maximum free energy costs are within +20.8 kcal mol$^{-1}$, corresponding to the formation of compounds $\mathbf{6'_{butyl}}$ and $\mathbf{6''_{butyl}}$, analogous to the initial adduct $\mathbf{6_{butyl}}$, and to the subsequent transition states

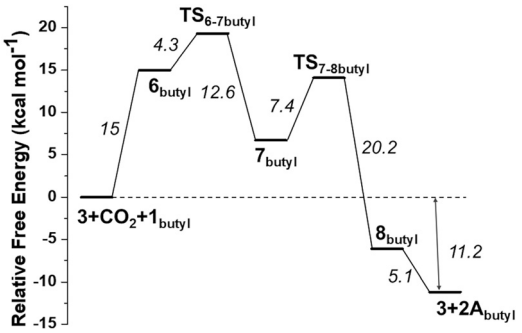


Fig. 5 Free energy (kcal mol$^{-1}$) pathway for the cycloaddition reaction of $CO_2$ to 1-butyl-2-phenyl aziridine $\mathbf{1_{butyl}}$ yielding 3-butyl-5-phenyloxazolidin-2-one $\mathbf{2A_{butyl}}$.

 This journal is © The Royal Society of Chemistry and the Centre National de la Recherche Scientifique 2025

Open Access Article. Published on 11 September 2025. Downloaded on 1/23/2026 4:32:47 PM. This article is licensed under a Creative Commons Attribution 3.0 Unported Licence.

$TS_{6'\text{-}7'butyl}$ and $TS_{6''\text{-}7''butyl}$. The energy barriers for $TS_{6'\text{-}7'butyl}$ and $TS_{6''\text{-}7''butyl}$ fall within the range of +6.2 to +9.2 kcal mol$^{-1}$. All the free energy values associated with the single step of the processes are listed in Fig. S2.

### Effect of the *N*-aziridine substituent on the reaction efficiency

Already published experimental data[40] highlighted that the steric and electronic nature of the substituent on the aziridine nitrogen center may drastically influence the reaction efficiency. No conversion was observed when 1-(3,5-*bis*(trifluoromethyl)phenyl)-2-phenyl aziridine ($\mathbf{1}_{aryl}$) was used in the $CO_2$ cycloaddition catalyzed by **3**. In contrast, when a cyclohexyl substituent was present at the nitrogen atom, the reaction proceeded with a low efficiency, affording the corresponding oxazolidin-2-one in 21% yield.[40] To clarify the influence of the substituent at the aziridine nitrogen atom on the reaction efficiency, DFT computational analysis was carried out. The study was run as already described for the reaction involving 1-butyl-2-phenylaziridine $\mathbf{1}_{butyl}$. First, two adducts with structures similar to that of $\mathbf{6}_{butyl}$ were optimized by reacting $CO_2$ and **3** either with 1-(3,5-*bis*(trifluoromethyl)phenyl)-2-phenylaziridine ($\mathbf{1}_{aryl}$) or 1-cyclohexyl-2-phenylaziridine ($\mathbf{1}_{cyhexyl}$), obtaining $\mathbf{6}_{aryl}$ and $\mathbf{6}_{cyhexyl}$ respectively. As shown in Fig. 6, the optimized structure of $\mathbf{6}_{aryl}$ displays an N2···C1 distance as large as 3.02 Å, as well as a very weak hydrogen bond between H($NH^+$) and O($CO_2$), with an H···O distance of 2.64 Å.

These features, together with the nearly unperturbed linear structure of the $CO_2$ moiety, suggest that the occurrence of the process is unlikely when an aryl substituent is present at the N2 aziridine center, in line with the experimental results. For this reason, the $CO_2$ cycloaddition to 1-(3,5-*bis*(trifluoromethyl)phenyl)-2-phenylaziridine was not investigated further. Conversely, when 1-cyclohexyl-2-phenylaziridine is the involved substrate, the adduct $\mathbf{6}_{cyhexyl}$ exhibits an activated $CO_2$ characterized by a bent O–C–O structure with an angle of 135° and a computed IR-active stretching at 1746 cm$^{-1}$. From the energy viewpoint, the formation of adduct $\mathbf{6}_{cyhexyl}$ requires a free energy cost of +19.2 kcal mol$^{-1}$, higher than that needed for achieving adduct $\mathbf{6}_{butyl}$ from 1-butyl-2-phenylaziridine (+15 kcal mol$^{-1}$). Even in this case, the obtained results are in line with experimental data, which highlighted a less efficient process when 1-cyclohexyl-2-phenylaziridine was employed as the starting material instead of 1-butyl-2-phenylaziridine.

The free energy barrier for conversion of $\mathbf{6}_{cyhexyl}$ to the transition state $TS_{6\text{-}7cyhexyl}$, whose optimized structure is reported in Fig. S3, is estimated to be +6.5 kcal mol$^{-1}$ while the overall energy barrier for transforming the starting reagents into $TS_{6\text{-}7cyhexyl}$ is +25.7 kcal mol$^{-1}$, a quite high value for a reaction performed at room temperature. The whole free energy associated with the formation of oxazolidin-2-one $\mathbf{2A}_{cyhexyl}$ from 1-cyclohexyl-2-phenylaziridine ($\mathbf{1}_{cyhexyl}$) and $CO_2$ is less exergonic than that of the same process involving 1-butyl-2-phenyl aziridine $\mathbf{1}_{butyl}$ (-7.5 kcal mol$^{-1}$ *versus* −11.2 kcal mol$^{-1}$). The complete energy profile of the $CO_2$ cycloaddition to 1-cyclohexyl-2-phenyl aziridine is reported in Fig. S4.

### Cycloaddition of $CS_2$ to 1-butyl-2-phenylaziridine ($\mathbf{1}_{butyl}$) promoted by cinchonine hydrochloride (3)

A precedent computational analysis has predicted the feasibility, at least *in silico*, of the $CS_2$ cycloaddition to *N*-alkyl aziridines to provide thiazolidin-2-thiones in the presence of bifunctional $\mathbf{TPPH_4Cl_2}$.[45] The study revealed a free energy contribution of −22.1 kcal mol$^{-1}$ associated with the cycloaddition of $CS_2$ to 1-butyl-2-phenylaziridine $\mathbf{1}_{butyl}$ to provide the corresponding thiazolidin-2-thione $\mathbf{9A}_{butyl}$.[45] Based on these results, we studied the reaction between $CS_2$ and 1-butyl-2-phenylaziridine $\mathbf{1}_{butyl}$ also in the presence of catalyst **3**. In this regard, the adduct $\mathbf{10}_{butyl}$ (Fig. 7) was optimized.

Despite the favorable enthalpic contribution of −2.1 kcal mol$^{-1}$, adduct $\mathbf{10}_{butyl}$ was optimized with a free energy cost of +21.5 kcal mol$^{-1}$. It should be noted that the energy cost is 6.5 kcal mol$^{-1}$ larger than that of the analogous process involving $CO_2$ (formation of adduct $\mathbf{6}_{butyl}$), possibly due to a weaker hydrogen bonding between the proton of **3** and the sulfur atom of $CS_2$, as confirmed by the long S–H distance of 2.28 Å.

After the formation of adduct $\mathbf{10}_{butyl}$, the activated aziridine substrate can be attacked by a chloride nucleophile through the transition state $TS_{10\text{-}11butyl}$ (Fig. 8) with a free energy barrier of +7.7 kcal mol$^{-1}$. The overall barrier of +29.2 kcal mol$^{-1}$ for the conversion of the reactants into $TS_{10\text{-}11butyl}$ was larger than that calculated for $CO_2$ activation and it can be overcome by performing the reaction at higher experimental temperatures.

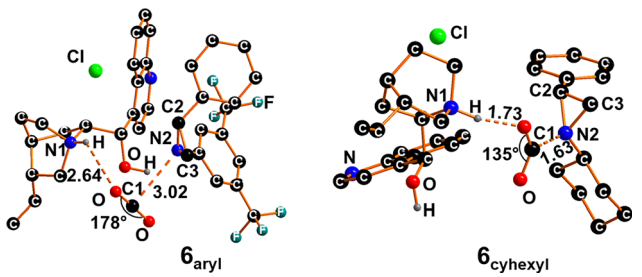


Fig. 6 Optimized structure of adducts $\mathbf{6}_{aryl}$ and $\mathbf{6}_{cyhexyl}$, presenting 1-(3,5-*bis*(trifluoromethyl)phenyl)-2-phenylaziridine and 1-cyclohexyl-2-phenylaziridine, respectively. The hydrogen atoms were hidden for the sake of clarity, except for those linked to a heteroatom. Selected distances are given in Å and O–C1–O angle in degrees (°).

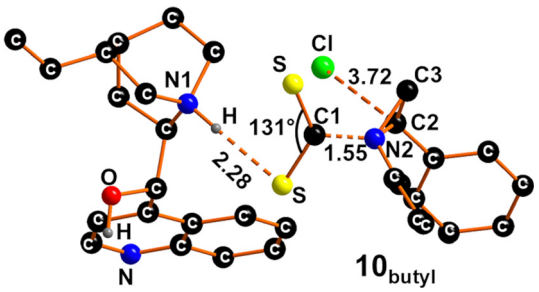


Fig. 7 Optimized structure of adduct $\mathbf{10}_{butyl}$. The hydrogen atoms were hidden for the sake of clarity, except for those linked to a heteroatom. Selected distances are given in Å and O–C1–O angle in degrees (°).

Open Access Article. Published on 11 September 2025. Downloaded on 1/23/2026 4:32:47 PM.
This article is licensed under a Creative Commons Attribution 3.0 Unported Licence.

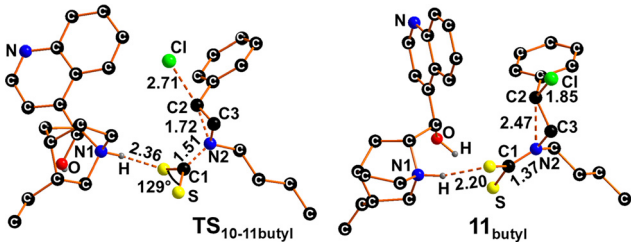


Fig. 8 Optimized structure of transition state $\mathbf{TS_{10\text{-}11butyl}}$ and of intermediate $\mathbf{11_{butyl}}$. The hydrogen atoms were hidden for the sake of clarity, except for those linked to a heteroatom. Selected distances are given in Å and O–C1–O angle in degrees (°).

Transition state $\mathbf{TS_{10\text{-}11butyl}}$ features a *quasi*-linear Cl–C2–N2 arrangement with an angle of 151° and a weakened C2–N2 bond, whose length is stretched by 0.15 Å compared to that in $\mathbf{10_{butyl}}$. In $\mathbf{TS_{10\text{-}11butyl}}$, the chloride approaches the C2 atom with a consistent shortening of Cl···C2 distance by 1.0 Å.

The complete formation of the C2–Cl bond in intermediate $\mathbf{11_{butyl}}$ (Fig. 8) was estimated to be exergonic by −25.9 kcal mol$^{-1}$.

Similar to the $CO_2$ activation, the sulfur atom in $\mathbf{11_{butyl}}$ may perform a nucleophilic attack on the C2 center to form the 5-membered ring and regenerate the catalyst **3**. The transition state $\mathbf{TS_{11\text{-}12butyl}}$, shown in Fig. S5, was obtained with a free energy barrier of +13.6 kcal mol$^{-1}$, while the intermediate $\mathbf{12_{butyl}}$ (Fig. 9) was obtained with the large free energy gain of −29.9 kcal mol$^{-1}$.

The complete release of thiazolidin-2-thione $\mathbf{9A_{butyl}}$, shown in Fig. 9, was achieved with a further free energy gain of −9.1 kcal mol$^{-1}$. The overall formation of compound $\mathbf{9A_{butyl}}$ by $CS_2$ cycloaddition to aziridine $\mathbf{1_{butyl}}$ is depicted in Fig. 10.

A comparison between the energy profiles of $CS_2$ (Fig. 10) and $CO_2$ (Fig. 5) cycloaddition to $\mathbf{1_{butyl}}$ reveals key differences. While a higher barrier is required for the formation of the initial adduct $\mathbf{10_{butyl}}$ and for reaching the transition state $\mathbf{TS_{10\text{-}11butyl}}$ in the case of $CS_2$ activation, more energy is released during $CS_2$ activation rather than during $CO_2$ activation. In summary, *in silico* analysis predicts that the energy barriers for the catalytic cycloaddition of $CS_2$ to aziridine rings are not prohibitively high, although temperatures above room temperature might be necessary to promote the reaction.

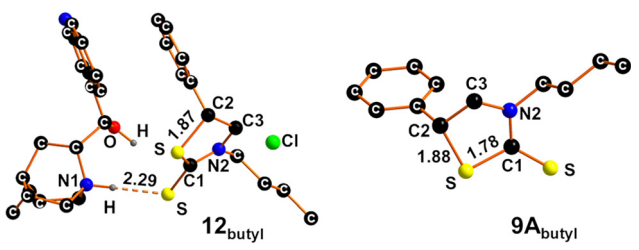


Fig. 9 Optimized structure of the intermediate $\mathbf{12_{butyl}}$ and thiazolidin-2-thione, $\mathbf{9A_{butyl}}$. The hydrogens were hidden for the sake of clarity, except for those linked to a heteroatom. Selected distances are given in Å and O–C1–O angle in degrees (°).

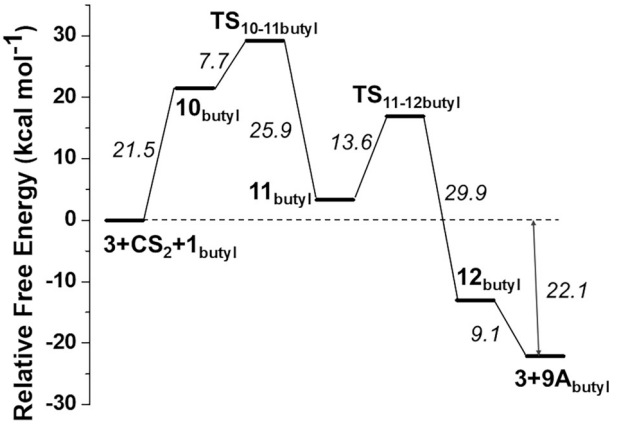


Fig. 10 Free energy (kcal mol$^{-1}$) pathway for the cycloaddition reaction of $CS_2$ to 1-butyl-2-phenyl aziridine $\mathbf{1_{butyl}}$ forming thiazolidin-2-thione $\mathbf{9A_{butyl}}$.

## Cycloaddition of COS to 1-butyl-2-phenylaziridine ($\mathbf{1_{butyl}}$) promoted by cinchonine hydrochloride (3)

Until now, only the activation of symmetric triatomic molecules has been investigated. This raises the question if the reaction can also proceed when a non-symmetric substrate, such as carbonyl sulfide COS, is used in the cycloaddition to aziridines.

Unlike previous cases, different structural isomers can be obtained starting from 1-butyl-2-phenylaziridine $\mathbf{1_{butyl}}$ and COS. Depending on which heteroatom is involved in the cyclization step, 3-butyl-5-phenylthiazolidin-2-one ($\mathbf{13A_{butyl}}$) or 3-butyl-5-phenyloxazolidin-2-thione ($\mathbf{14A_{butyl}}$) can be formed (Fig. 11).

To begin the computational analysis of the reaction between COS and $\mathbf{1_{butyl}}$, both compounds shown in Fig. 11 were optimized. Isomers $\mathbf{13B_{butyl}}$ and $\mathbf{14B_{butyl}}$, derived from the nucleophilic attack to the less electrophilic carbon atom C3 of the aziridine ring, were not theoretically modelled in view of the unfavorable energy costs related to their formation (see below).

Preliminary DFT calculations revealed that product $\mathbf{13A_{butyl}}$ is more stable than $\mathbf{14A_{butyl}}$ by 10.4 kcal mol$^{-1}$ in free energy. Although the energy difference between the two potential products is significant, the processes yielding both isomers were investigated. Given the non-symmetrical nature of COS, both adducts $\mathbf{15_{butyl}}$ (evolving in $\mathbf{13A_{butyl}}$) and $\mathbf{16_{butyl}}$ (evolving in $\mathbf{14A_{butyl}}$) (Fig. 12) were optimized, featuring the alternative involvement of either oxygen or sulfur in hydrogen bonding, respectively. Adduct $\mathbf{15_{butyl}}$ was estimated to be 1.3 kcal mol$^{-1}$

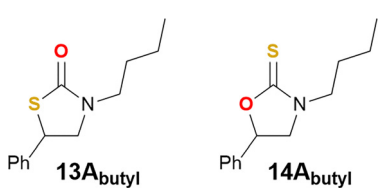


Fig. 11 Potential products of the cycloaddition of COS to 1-butyl-2-phenylaziridine ($\mathbf{1_{butyl}}$).

 This journal is © The Royal Society of Chemistry and the Centre National de la Recherche Scientifique 2025

Open Access Article. Published on 11 September 2025. Downloaded on 1/23/2026 4:32:47 PM.
This article is licensed under a Creative Commons Attribution 3.0 Unported Licence.

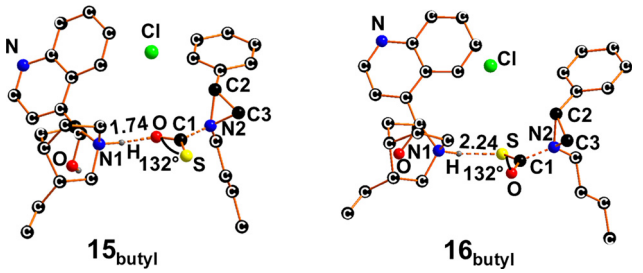


Fig. 12 Free energy (kcal mol$^{-1}$) pathway for the cycloaddition reaction of $CS_2$ to 1-butyl-2-phenyl aziridine $\mathbf{1_{butyl}}$ forming thiazolidin-2-thione $\mathbf{9A_{butyl}}$. Selected distances are given in Å and O–C1–O angle in degrees (°).

more stable than $\mathbf{16_{butyl}}$, mainly due to more efficient hydrogen bonding when oxygen, rather than sulfur, is involved.

Starting from the reactants, adduct $\mathbf{15_{butyl}}$ is obtained with a free energy cost of +15.9 kcal mol$^{-1}$, while the formation of $\mathbf{16_{butyl}}$ requires a slightly higher cost of +17.2 kcal mol$^{-1}$. For adduct $\mathbf{15_{butyl}}$, the N2–C2 bond cleavage *via* nucleophilic attack of chloride proceeds through transition state $\mathbf{TS_{15\text{-}17butyl}}$ (Fig. S6) with an associated free energy barrier of +5.8 kcal mol$^{-1}$. The system then evolves toward intermediate $\mathbf{17_{butyl}}$ (Fig. 13), with a free energy gain of −16.7 kcal mol$^{-1}$. Accordingly, an overall energy barrier of +21.7 kcal mol$^{-1}$ must be overcome to reach $\mathbf{TS_{15\text{-}17butyl}}$ from the separate reactants.

Accordingly, an overall energy barrier of +21.7 kcal mol$^{-1}$ must be overcome to reach $\mathbf{TS_{15\text{-}17butyl}}$ from the separate reactants. The potential nucleophilic attack of chloride on the C3 center has been also investigated highlighting a free energy barrier of +17.8 kcal mol$^{-1}$ to obtain $\mathbf{TS_{15\text{-}17butylC3}}$, shown in Fig. S6, from adduct $\mathbf{15_{butyl}}$. Since the overall estimated free energy barrier for reaching $\mathbf{TS_{15\text{-}17butylC3}}$ is as high as +33.7 kcal mol$^{-1}$, this mechanism was discarded.

In the case of adduct $\mathbf{16_{butyl}}$, where the sulfur atom is involved in hydrogen bonding, the estimated free energy barrier for reaching $\mathbf{TS_{16\text{-}18butyl}}$ is +11.5 kcal mol$^{-1}$, resulting in an overall barrier of +28.7 kcal mol$^{-1}$ from the isolated reactants to $\mathbf{TS_{16\text{-}18butyl}}$. The system then proceeds to intermediate $\mathbf{18_{butyl}}$,

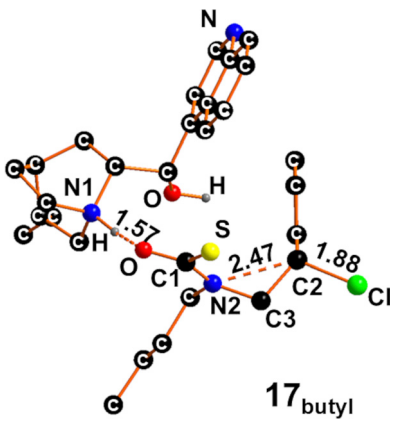


Fig. 13 Optimized structure of the intermediate $\mathbf{17_{butyl}}$. The hydrogens were hidden for the sake of clarity, except for those linked to a heteroatom center. Selected distances are given in Å and O–C1–O angle in degrees (°).

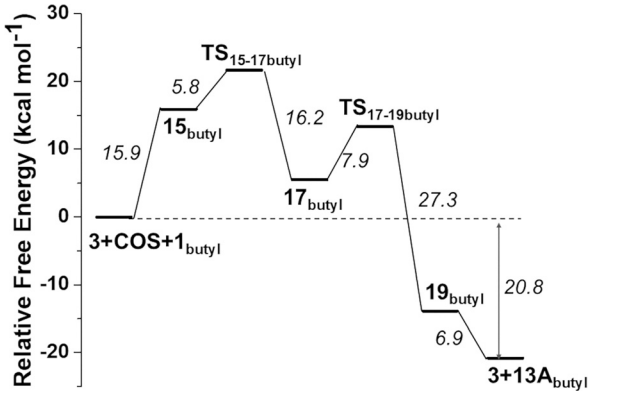


Fig. 14 Free energy (kcal mol$^{-1}$) pathway for the cycloaddition reaction of COS to 1-butyl-2-phenyl aziridine $\mathbf{1_{butyl}}$ forming $\mathbf{13A_{butyl}}$.

with a free energy gain of −25.4 kcal mol$^{-1}$. Thus, in view of the quite high calculated barrier compared to that of $\mathbf{TS_{15\text{-}17butyl}}$, the energy pathway for the formation of $\mathbf{14A_{butyl}}$ was discarded.

Starting from $\mathbf{17_{butyl}}$, the transition state $\mathbf{TS_{17\text{-}19butyl}}$ was computed with a free energy barrier of +7.9 kcal mol$^{-1}$, in which the sulfur center of COS can perform a nucleophilic attack to the C2 center yielding the intermediate $\mathbf{19_{butyl}}$ that evolves into the final product 3-butyl-5-phenylthiazolidin-2-one $\mathbf{13A_{butyl}}$. The complete release of $\mathbf{13A_{butyl}}$ and restoration of catalyst **3** is accompanied by a free energy gain of −6.9 kcal mol$^{-1}$. A complete free energy pathway for the production of 3-butyl-5-phenylthiazolidin-2-one $\mathbf{13A_{butyl}}$, starting from COS and aziridine $\mathbf{1_{butyl}}$ promoted by metal-free **3**, is depicted in Fig. 14 and shows an overall free energy gain of −20.8 kcal mol$^{-1}$.

To better summarize and compare the reactivity of the investigated triatomic molecules, the energy profiles of their cycloaddition to 1-butyl-2-phenyl aziridine $\mathbf{1_{butyl}}$ catalyzed by **3** were superimposed, as shown in Fig. 15.

A clear difference in overall energy gains can be observed between the formation of oxazolidine-2-one $\mathbf{2A_{butyl}}$ and its sulfur-containing analogues ($\mathbf{9A_{butyl}}$ and $\mathbf{13A_{butyl}}$). The overall

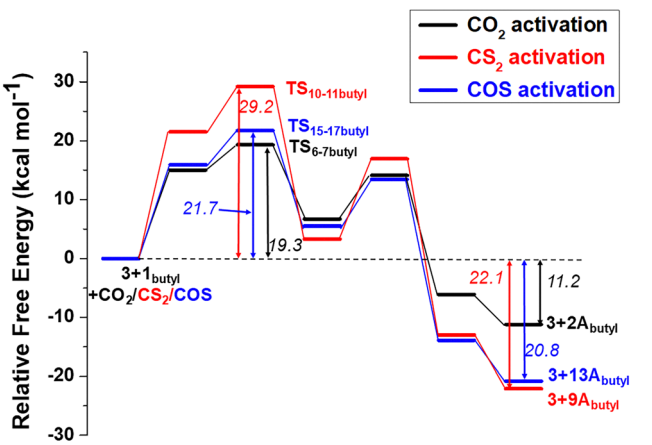


Fig. 15 Superimposed free energy (kcal mol$^{-1}$) profiles of the cycloaddition reaction of $CO_2$, COS and $CS_2$ to 1-butyl-2-phenyl aziridine $\mathbf{1_{butyl}}$ catalyzed by **3**.

Open Access Article. Published on 11 September 2025. Downloaded on 1/23/2026 4:32:47 PM.
This article is licensed under a Creative Commons Attribution 3.0 Unported Licence.

energy gains calculated for $CS_2$ and COS cycloaddition to $\mathbf{1_{butyl}}$ were nearly twice as high as that for $CO_2$ ($-20.8$ kcal mol$^{-1}$ and $-22.1$ kcal mol$^{-1}$ *versus* $-11.2$ kcal mol$^{-1}$), suggesting a thermodynamic preference for the formation of oxazolidin-2-thiones and thiazolidin-2-thiones over oxazolidin-2-ones.

However, the activation barrier computed for the formation of the key transition state was higher for $CS_2$ (+29.2 kcal mol$^{-1}$) compared to $CO_2$ (+19.3 kcal mol$^{-1}$), indicating that more forcing reaction conditions may be required to achieve the product formation. In contrast, the energy barrier to reach the first transition state from COS is only slightly larger than that calculated for $CO_2$ (+21.7 kcal mol$^{-1}$ *versus* +19.3 kcal mol$^{-1}$), suggesting that its cycloaddition could proceed efficiently under the similar mild conditions successfully employed for the **3**-catalyzed oxazolidin-2-one synthesis. These findings support the feasibility of COS cycloaddition to aziridines promoted by catalyst **3** under experimental conditions only slightly more drastic than those validated for $CO_2$ transformations.

## Conclusions

In conclusion, the energetic/structural DFT analyses suggest a mechanism for the $CO_2$ cycloaddition to the aziridine ring for the synthesis of oxazolidin-2-ones, efficiently promoted by cinchonine hydrochloride **3** under very mild conditions (RT and 0.1 MPa of $CO_2$ pressure). The calculated energy barriers are compatible to the employed experimental conditions and the DFT study confirmed the double activation of $CO_2$ through hydrogen bonding interactions and nucleophile attack of the aziridine nitrogen atom to the $CO_2$ carbon atom. The theoretical analysis explains the dependence of the catalytic efficiency on the steric hindrance and/or electronic effects of the *N*-aziridine substituents, providing a rationale for the lack of reactivity of *N*-aryl aziridines, observed experimentally.

To extend the activation of triatomic molecules mediated by **3** from $CO_2$ to $CS_2$ and COS, the DFT study reported here will be fundamental for managing in near future experimental reactions involving $CS_2$ and COS, which until now have only been theoretically predicted. The computational analysis revealed that catalyst **3** could be a potential candidate for efficiently mediating both $CS_2$ and COS activation. Even if theoretical calculations underlined that both processes involve higher energy barriers than those optimized for the $CO_2$ activation, acquired data support a future experimental study on the $CS_2$ and COS cycloaddition to aziridine in the presence of **3**. By comparing the calculated energy barriers, the cycloaddition of COS is predicted to be feasible at temperatures close to the ambient one, under conditions therefore similar to those observed for the **3**-catalyzed valorization of $CO_2$. In contrast, the use of $CS_2$ would require slightly higher temperatures. In both cases, the synthesis of thiazolidin-2-thiones and oxazolidin-2-thiones is predicted to be feasible using an inexpensive and biocompatible catalyst, such as cinchonine hydrochloride salt (**3**), under mild reaction conditions.

## Conflicts of interest

There are no conflicts to declare.

## Data availability

The datasets supporting this article are included in the SI. See DOI: **https://doi.org/10.1039/d5nj03189c**.

Additional data are available from the corresponding author upon reasonable request.

## Acknowledgements

CD and EG thank Università degli Studi di Milano for the PSR 2023 grants. GM acknowledges the CINECA award under the ISCRA initiative, for the availability of high-performance computing resources and support.

## References

1 X. B. Li, Z. K. Xin, S. G. Xia, X. Y. Gao, C. H. Tung and L. Z. Wu, *Chem. Soc. Rev.*, 2020, **49**, 9028–9056.
2 L. Wang, W. Chen, D. Zhang, Y. Du, R. Amal, S. Qiao, J. Wu and Z. Yin, *Chem. Soc. Rev.*, 2019, **48**, 5310–5349.
3 D. Intrieri, C. Damiano, P. Sonzini and E. Gallo, *J. Porphyrins Phthalocyanines*, 2019, **23**, 305–328.
4 C. Damiano, M. Cavalleri, L. Invernizzi and E. Gallo, *Eur. J. Org. Chem.*, 2024, e202400616.
5 T. Yan, H. Liu, Z. X. Zeng and W. G. Pan, *J. CO2 Util.*, 2023, **68**, 102355.
6 K. Wiranarongkorn, K. Eamsiri, Y. S. Chen and A. Arpornwichanop, *J. CO2 Util.*, 2023, **71**, 102477.
7 L. Li, X. Li, Y. Sun and Y. Xie, *Chem. Soc. Rev.*, 2022, **51**, 1234–1252.
8 L. Rotundo, R. Gobetto and C. Nervi, *Curr. Opin. Green Sustainable Chem.*, 2021, **31**, 100509.
9 Q. Zhang and X. Jin, *Chem. – Eur. J.*, 2025, **31**, e202500933.
10 M. Aresta, A. Dibenedetto and E. Quaranta, *J. Catal.*, 2016, **343**, 2–45.
11 S. Kaewsai and V. D' Elia, *J. Organomet. Chem.*, 2025, **1039**, 123799.
12 W. Natongchai, D. Crespy and V. D' Elia, *Chem. Commun.*, 2025, **61**, 419.
13 S. Arayachukiat, P. Yingcharoen, S. V. C. Vummaleti, L. Cavallo, A. Poater and V. D'Elia, *Molecular Catalysis*, 2017, **443**, 280–285.
14 P. Yingcharoen, W. Natongchai, A. Poater and V. D' Elia, *Catal. Sci. Technol.*, 2020, **10**, 5544–5558.
15 C. Damiano, P. Sonzini, G. Manca and E. Gallo, *Eur. J. Org. Chem.*, 2021, 2807–2814.
16 M. Cavalleri, C. Damiano, G. Manca and E. Gallo, *Chem. – Eur. J.*, 2023, **29**, e202202729.
17 C. Damiano, P. Sonzini, M. Cavalleri, G. Manca and E. Gallo, *Inorg. Chim. Acta*, 2022, **540**, 121065.
18 P. Sonzini, C. Damiano, D. Intrieri, G. Manca and E. Gallo, *Adv. Synth. Catal.*, 2020, **362**, 2961–2969.

 This journal is © The Royal Society of Chemistry and the Centre National de la Recherche Scientifique 2025

Open Access Article. Published on 11 September 2025. Downloaded on 1/23/2026 4:32:47 PM.
This article is licensed under a Creative Commons Attribution 3.0 Unported Licence.

19 P. Sonzini, N. Berthet, C. Damiano, V. Dufaud and E. Gallo, *J. Catal.*, 2022, **414**, 143–154.
20 C. Damiano, A. Fata, M. Cavalleri, G. Manca and E. Gallo, *Catal. Sci. Technol.*, 2024, **14**, 3996–4006.
21 A. Z. Bialvaei, M. Rahbar, M. Yousefi, M. Asgharzadeh and H. S. Kafil, *J. Antimicrob. Chemother.*, 2017, **72**, 354–364.
22 D. McBride, T. Krekel, K. Hsueh and M. J. Durkin, *Expert Opin. Drug Metab. Toxicol.*, 2017, **4**, 491.
23 F. Moureau, J. Wouters, D. Vercauteren, S. Collin, G. Evrard, F. Durant, F. Ducrey, J. Koenig and F. Jarreau, *Eur. J. Med. Chem.*, 1992, **27**, 939–948.
24 G. Bresciani, M. Bortoluzzi, G. Pampaloni and F. Marchetti, *Org. Biomol. Chem.*, 2021, **19**, 4152–4161.
25 C. S. Dewey and R. A. Bafford, *J. Org. Chem.*, 1965, **30**, 491–495.
26 T. A. Foglia, L. M. Gregory, G. Maerker and S. F. Osman, *J. Org. Chem.*, 1971, **36**, 1068–1072.
27 K. K. Pandey, *Coord. Chem. Rev.*, 1995, **140**, 37–114.
28 M. Guo, B. Dong, Y. Qu, Z. Sun, L. Yang, Y. Wang, I. L. Fedushkin and X. J. Yang, *Chem. – Eur. J.*, 2025, **31**, e202403652.
29 Y. Xie, C. Lu, B. Zhao, Q. Wang and Y. Yao, *J. Org. Chem.*, 2019, **84**, 1951–1958.
30 Y. Shi, D. Wen and S. Q. Zhao, *Inorg. Chem.*, 2025, **64**, 4387–4392.
31 W. Ding, X. Tang, S. Jin, Z. Li, D. Xu, X. Kang and Z. Liu, *Green Chem.*, 2024, **27**, 218–226.
32 Y. Shi, B. Tang, X.-L. Jiang, Y.-E. Jiao, H. Xu and B. Zhao, *J. Mater. Chem. A*, 2022, **10**, 4889–4894.
33 A. J. Plajer and C. K. Williams, *Angew. Chem., Int. Ed.*, 2022, **61**, e2021044952022.
34 K. Sieja, J. von Mach-Szczypiński and J. von Mach-Szczypiński, *Med. Pr.*, 2018, **69**, 317–323.
35 A. W. Demartino, D. F. Zigler, J. M. Fukuto and P. C. Ford, *Chem. Soc. Rev.*, 2017, **46**, 21–39.
36 R. Morales-Nava, M. Fernández-Zertuche and M. Ordóñez, *Molecules*, 2011, **16**, 8803–8814.
37 A. Khalaj and M. Khalaj, *J. Chem. Res.*, 2016, **40**, 445–448.
38 A. Biswas and S. Hajra, *Adv. Synth. Catal.*, 2022, **364**, 3035–3042.
39 M. Sengoden, G. A. Bhat and D. J. Darensbourg, *Green Chem.*, 2022, **24**, 2535–2541.
40 L. Invernizzi, C. Damiano and E. Gallo, *Chem. – Eur. J.*, 2025, **31**, e202500473.
41 S. Grimme, *J. Comp. Chem.*, 2006, **27**, 1787–17991.
42 V. Barone and M. Cossi, *J. Phys. Chem. A*, 1998, **102**, 1995–20013.
43 M. Cossi, N. Rega, G. Scalmani and V. Barone, *J. Comp. Chem.*, 2003, **24**, 669–681.
44 L. R. Domingo, M. Ríos-Gutiérrez and P. Pérez, *Molecules*, 2016, **21**, 7482016.
45 C. Damiano, N. Panza, J. Nagy, E. Gallo and G. Manca, *New J. Chem.*, 2023, **47**, 4306–4312.